Evolutionary engineering improved D-glucose/xylose co-fermentation of Yarrowia lipolytica

Journal:	*Industrial & Engineering Chemistry Research*
Manuscript ID	ie-2020-008963.R2
Manuscript Type:	Article
Date Submitted by the Author:	n/a
Complete List of Authors:	Zhou, Linlin; Nanjing University of Science and Technology, School of Environmental and Biological Engineering Wen, Zhiqiang; Nanjing University of Science and Technology, School of Environmental and Biological Engineering Wang, Zedi; Nanjing University of Science and Technology, School of Environmental and Biological Engineering Zhang, Yuwei; Nanjing University of Science and Technology, School of Environmental and Biological Engineering Ledesma-Amaro, Rodrigo; Imperial College London, Department of Bioengineering Jin, Mingjie; Nanjing University of Science and Technology, School of Environmental and Biological Engineering

Evolutionary engineering improved D-glucose/xylose co-fermentation of *Yarrowia lipolytica*

Linlin Zhou[1], Zhiqiang Wen[1*], Zedi Wang[1], Yuwei Zhang[1], Rodrigo Ledesma-Amaro[2], Mingjie Jin[1*]

[1] School of Environmental and Biological Engineering, Nanjing University of Science & Technology, Nanjing, 210094, China
[2] Department of Bioengineering, Imperial College London, London SW7 2AZ, UK

*Corresponding authors: Mingjie Jin, E-mail: jinmingjie@njust.edu.cn (ORCID: 0000-0002-9493-305X); Zhiqiang Wen, E-mail: zqwen@njust.edu.cn (ORCID: 0000-0001-8083-7588)

Abstract: The recombinant strain *Y. lipolytica* XYL+ can utilize xylose to produce microbial lipid efficiently. However, its xylose uptake is severely delayed in the presence of D-glucose. In this study, adaptive laboratory evolution (ALE) of strains in the medium containing xylose and D-glucose analog 2-deoxyglucose (dG) is performed. After four stages of evolution over a total of 64 days, for the first time, we obtained an *Y. lipolytica* strain (yl-XYL+*04*10) that can co-metabolize xylose and glucose, with diminished glucose repression. Xylose uptake kinetics showed that it could efficiently utilize xylose in the presence of 10 g/L dG or D-glucose. Transcriptional profiling analysis revealed that relative expression level of xylose-specific transporter genes (encoded by YALI0_C04730g and YALI0_D00363g) was significantly up-regulated. Besides, missense mutations N373T and G270A in YALI0_E23287g (encoding a D-glucose transporter) and YALI0_E15488g (encoding a hexokinase) respectively, were found. It implied that these are important gene targets responsible for improved xylose utilization in evolved *Y. lipolytica.* Our work provides a new approach for breeding *Y. lipolytica* and paved the way for future pentose metabolic engineering.

Keywords: *Yarrowia lipolytica*, 2-deoxyglucose, adaptive laboratory evolution, transcriptome analysis, xylose-specific transporter

1. INTRODUCTION

Yarrowia lipolytica is a well-known ascomycetous yeast for its safety (generally recognized as safe (GRAS)) and broad applications [1]. It has been used in the field of organic acids production (citrate, isocitrate, alpha-ketoglutarate, pyruvate and succinate) [2], pollutants degradation [3], food additives synthesis (hydrophobic terpenoids) [4], and enzymes expression [5]. In particular, it is an emerging oleaginous yeast factory, due to its strong acetyl-CoA and malonyl-CoA flux as well as the availability of facile genetic manipulation tools [6, 7]. Although some model organisms have also been converted into oleaginous organisms by genetic engineering [8, 9] (for example, *S. cerevisiae* has been engineered to be able to accumulate up to 33.4 g/L lipid [10]), the lipid production capacity is much lower compared to *Y. lipolytica* [11-13]. Recently, Xu and Qiao et al. rewired fatty acyl-CoA and fatty acyl-ACP metabolism in the cytoplasm, peroxisome, or endoplasmic reticulum, and cytosolic redox metabolism. Their best engineered strain produced 98.9 g/L of fatty acid methyl esters with a productivity of 1.2 g/L/h and a process yield of 0.27 g/g-glucose [11, 12]. When the carbon source was changed from glucose to acetate, triacylglyceride production could be improved to 115 g/L in bench-top bioreactors[13]. It represents a milestone toward commercialization of microbial lipid production.

Abundant and cheap lignocellulosic biomass are ideal feedstock for large-scale production of microbial lipid. Accordingly, it is of crucial importance to enable *Y. lipolytica* uptake and metabolize xylose efficiently, because xylose is the second most abundant sugar in the lignocellulosic hydrolysates [14]. Unfortunately, wild *Y. lipolytica* can hardly utilize xylose, which may reduce the oleochemicals yield from lignocellulosic biomass. Interestingly, *Y.lipolytica* has been experimentally confirmed to harbor endogenous xylose-specific transporters YALI0_C04730 and YALI0_B00396 as well as complete xylose metabolic pathways, including XYR (xylose reductase, YALI0_D07634), XDH (xylitol dehydrogenase, YALI0_E12463) and XKS (xylulokinase, YALI0_F10923) [15-17]. At present, some xylose metabolic engineering of *Y. lipolytica* attempted to engineer a native or hybrid pathway [15, 18-21], but these recombinant strains exhibited a carbon catabolite repression (CCR) in mixed sugars medium, in which, xylose consumption is severely inhibited by D-glucose. The phenomenon is common in most microorganisms [22], which may be attributed to the low efficiency of xylose transporters, complex regulation of metabolism, and the un-fluent pentose phosphate pathway [15, 16, 18-21]. However, CCR can be relieved or even eliminated by metabolic and evolutionary engineering [23, 24].

Previous studies have found that strains that can utilize xylose in the presence of D-glucose homologues (structurally similar to D-glucose but not metabolizable), can co-ferment D-glucose/xylose without obvious preference [25-29]. Adaptive laboratory evolution of strains in a medium composing of xylose and the D-glucose analog 2-deoxyglucose (hereafter abbreviated as dG) has been adapted to obtain mutants with derepressed pentose metabolism. It has been proved successful in recombinant *Saccharomyces cerevisiae*, *Pichia stipitis*, *Zymomonas mobilis*, *Thermoanaerobacterium saccharolyticum* among others [25-29]. Kahar et al. found that the evolved strain showed more than 4-fold higher xylose uptake in the presence of D-

glucose than the wild strain [29]. In vitro analyses of the key evolved enzymes showed higher metabolic activities in the pentose phosphate pathway [29]. In another study, Lane et al. re-sequenced the evolved mutant and performed a reverse engineering to verify the putative gene targets [25]. In that case, mutations in D-glucose phosphorylating enzymes (Hxk1, Hxk2, Glk1) were responsible for the simultaneous D-glucose and xylose utilization. Unexpectedly, no mutations in sugar transporters were detected [25]. More recently, Li et al. found that the strain mating can obtain xylose-utilizing strains, which can produce biomolecules from xylose with higher production level than the parental strain [30]. Although improved phenotype in D-glucose/xylose co-fermentation of evolved strains have been investigated by fermentation kinetics, enzymology, resequencing and reverse metabolic engineering, the exact underlying mechanism has not been fully understood [25-27, 31].

Recently, Ledesma-Amaro et al. overexpressed xylose reductase and xylitol dehydrogenase from *Scheffersomyces stipitis* and endogenous xylulokinase in *Y. lipolytica* strain Po1d (a derived strain of wild type W29), generating a recombinant strain yl XYL+ (collection number: JMY5610) [18]. yl XYL+ can uptake xylose efficiently and its growth in xylose is comparable with that of the wild type in D-glucose. However, yl XYL+ still preferred D-glucose. Xylose metabolism is severely inhibited until D-glucose is exhausted. The inability to co-ferment D-glucose and xylose has become one of the major obstacles for further development of *Y. lipolytica* as industrial microbial chassis [17, 18].

In this study, we would like to further improve the recombinant strain yl-XYL+ to co-ferment both sugar since it can be very valuable for the industry. Therefore, adaptive laboratory evolution (ALE) of strains with D-glucose analog 2-deoxyglucose (dG) is performed, as shown in Figure 1. We carried out a four-stage dG tolerant evolution experiment, in which the concentration of 2-dG was gradually increased from 1 g/L to 2, 5 and 10 g/L. One mutant was screened at the end of each stage, generating the evolved strains named as yl-XYL+*01*3, yl-XYL+*02*9, yl-XYL+*03*5 and yl-XYL+*04*10, respectively. Phenotype characterization and kinetics test showed that yl-XYL+*04*10 consumed xylose efficiently in presence of 10 g/L of D-glucose. Transcriptional analysis of yl-XYL+, yl-XYL+*01*3, yl-XYL+*04*10 revealed that YALI0_C04730g and YALI0_D00363g encoding xylose-specific transporters, and missense mutations N373T and G270A in YALI0_E23287g (encoding a D-glucose transporter) and YALI0_E15488g (encoding a hexokinase) respectively, which might be related with the improved phenotype in co-fermentation. Our work provides a new approach for breeding *Y. lipolytica* and paved the way for future pentose metabolic engineering.

2. RESULTS

2.1. Adaptive laboratory evolution of recombinant strain *Y. lipolytica* XYL+

2.1.1. Setting up the right conditions for evolution

To perform D-glucose analog 2-deoxyglucose (hereafter abbreviated as dG) tolerance evolution to the yl-XYL+, we firstly test the toxicity of dG to confirm the initial condition of evolution. dG is toxic to yl-XYL+ in both $YNBdG_{10}$ medium (dG as sole carbon source) and $YNBdG_{10}X_{10}$ medium (with dG and xylose as carbon sources). It caused 88.8% and 100% death of yl-XYL+ in $YNBdG_{10}$ medium within 24 and 32 h, respectively, while in $YNBdG_{10}X_{10}$ medium, it resulted in 50.9% and 58.9% death (Figure 2A). This suggested that dG blocked xylose transportation or metabolism, but it was not totally lethal to yl-XYL+, which made it possible to drive yl-XYL+ evolution to consume xylose in $YNBdG_{10}X_{10}$ medium.

After confirming that dG inhibited the xylose metabolism of the yl-XYL+, a small amount of D-glucose was added to the $YNBdG_xX_{10}$ medium to help yl-XYL+ grow to a baseline biomass so that it can evolve to uptake xylose in the presense of dG. Impacts of different D-glucose addition were investigated in Figure 2B, it was found that 2 g/L of D-glucose can ensure that the yl-XYL+'s growths to about 1.0 of OD_{600} within 24 h, which basically satisfied a baseline biomass requirement. Then we investigated how much xylose could be consuming within 24 h when the baseline biomass was set as 1.0 of OD_{600}. We found that the original strain could consume 10 g/L xylose within 24 h with an initial OD_{600} at 1.0 (Figure 2C). To further confirm this result, we tested the consumption of 10 g/L xylose in 24 h with different initial inoculum size (Figure 2D). It was also found that baseline biomass at 1.0 of OD_{600} could consume 10 g/L xylose, while less inoculum could not. Therefore, the initial conditions of evolution were set as follows: the concentrations of dG, D-glucose, and xylose were 1, 2, and 10 g/L in the YNB medium, respectively; the evolution period was 48 h (determined after tests), in which, the first 24 hours were assumed to be a proliferative period (using D-glucose as carbon source) and the second 24 hours were assumed to be the evolution period (using xylose as sole carbon source in the presence of dG).

2.1.2. Adaptive laboratory evolution selects strains with the capacity of consuming xylose

Based on the above initial conditions, we started an adaptive laboratory evolution of yl-XYL+. The evolution went through four stages for a total of 64 days, as shown in Figure 3A. It shows the measured biomass (OD_{600}) and residual xylose in $YNBD_2dG_xX_{10}$ medium. When residual xylose concentration is less than 0.5 g/L, an evolution stage is ended. The evolution conditions remain unchanged except dG concentration increasing from 1 g/L to 2, 5 and 10 g/L in stage 1, 2, 3 and 4. In stage 1, overall increasing biomass and decreasing residual xylose are observed, which implies that the strains have evolved to utilize xylose at the presence of 1 g/L of dG. Evolution of stage 1 completed on 20th days and the culture populations from the last batch were harvested and spread on solidified medium for clones selection and phenotype test. Strain yl-XYL+*01*3 with best growth and xylose consumption phenotype was selected from ten randomly colonies picked up from the plate (Figure S1A), and was used for subsequent evolution. Strains yl-XYL+*02*9, yl-XYL+*03*5 and yl-XYL+*04*10 were obtained in the same way (Figure S1B, C and D).

2.1.3. Qualitative characterization of domesticated strains

At the end of each round of domestication, one of the best colonies was selected for the next round of domestication. After 4 rounds of domestication, we obtained 4 domesticated strains, which have a closely derivative relationship with high values to be characterized and compared with each other. dG tolerance of the domesticated and control strains was evaluated. The domesticated strain and the control strain were spread on various solid mediums including $YNBdG_1$, $YNBdG_1X_{10}$, $YNBD_{10}X_{10}$ and $YNBX_{10}$, respectively (Figure S2A). It is obvious that the evolved strains can grow on $YNBdG_1X_{10}$ medium, but the original strain yl-XYL+ cannot. As expected, strains with stronger dG resistance showed better growth phenotype in $YNBdG_1/X_{10}$ medium. Morphology of parent and evolved strains in optical microscope was also investigated, but no obvious difference was observed (Figure S2B).

Since the domesticated strain can grow well with xylose as carbon source in the presence of dG, we examined the fermentation performance of the domesticated strain in $YNBD_{15}X_{15}$ medium. The samples were taken at 24 h and 36 h. As shown in Figure 3B, the evolved strains can utilize significant amounts of xylose in the presence of D-glucose, the parental strain barely uses it. Nonetheless, the level of D-glucose utilization seems to be impaired in all evolved strains. Overall, all the evolved strains can utilize xylose in the presence of D-glucose or dG, which indicated that they can ferment D-glucose and xylose simultaneously. In addition, the more evolved strains performed better than the less evolved ones.

2.2. Evolved strains can simultaneously uptake D-glucose and xylose

2.2.1. Fermentation phenotype

In order to understand the fermentation performance of the domesticated strain, the strains yl-XYL+, yl-XYL+*01*3 and yl-XYL+*04*10 were grown in different medium in order to systematically investigated xylose and D-glucose consumption (Figure 4). In pure xylose medium, xylose utilizations and biomass of all strains were almost identical (Figure 4B, E and H). With D-glucose as sole carbon source, yl-XYL+*01*3 showed similar phenotype with the original strain yl-XYL+, but yl-XYL+*04*10 exhibited 10.19% and 9.78% decrease compared to yl-XYL+ and yl-XYL+*01*3 in the first 12 h, respectively (Figure 4A, D and G). Similar to glucose utilization, the final biomass production of yl-XYL+*04*10 exhibited 13.9% and 8.7% decrease compared to yl-XYL+ and yl-XYL+*01*3, respectively (Figure 4A, D and G).

When the mixed sugars were fermented, all domesticated strains were able to utilize xylose in the presence of D-glucose at concentration over 25 g/L, while the original strain yl-XYL+ could not until D-glucose was exhausted. As shown in the third column of Figure 4C, F and I, it is obvious that yl-XYL+*04*10 showed better co-fermentation performance than yl-XYL+*01*3, and yl-XYL+*01*3 performed much better than yl-XYL+. Interestingly, in the first 24 h, average xylose utilization rates of the evolved strains in the mixed sugar fermentation were enhanced by 131% and 105%

compared to the original strain, but their D-glucose utilization rate was decreased by 28.0% and 24.6%. Moreover, through linear fitting, there was a linear correlation between the increase of total sugar utilization and the increase of biomass (R^2> 0.94). However, the linear relationships between the biomass and sugar consumption of the evolved strain and the original strain had no significant difference (Figure S6). These suggests that the simultaneous fermentation might be achieved in a manner that weakened D-glucose uptake but enhanced xylose utilization.

2.2.2. Xylose uptake kinetics in the presence of dG and D-glucose

In order to investigate whether the xylose uptake became stronger and the D-glucose uptake became weaker during the fermentation of the mixed sugar, we carried out kinetic studies in both YNBdG$_x$X$_x$ medium and YNBD$_x$X$_x$ medium, as depicted in Table 1 and Figure 5. 1 g/L of dG almost completely inhibited xylose uptake of yl-XYL+ (Figure 5A); while for yl-XYL+*01*3, 1 g/L of dG had no effect. 2 g/L of dG only inhibited less than 30% of its xylose uptake rate. 5 g/L and 10 g/L dG severely inhibited and even completely eliminated xylose uptake (Figure 5B); As for yl-XYL+*04*10, 5 g/L and 10 g/L of dG inhibited the uptake rate by 53.6% and 56.3% respectively when using 30 g/L of xylose (Figure 5C). Inhibition of xylose uptake by D-glucose on parent and evolved strains show a similar pattern. 1 g/L D-glucose can completely inhibit xylose uptake of yl-XYL+, which explained why yl-XYL+ cannot utilize xylose in the presence of D-glucose (Figure 5D). 10 g/L D-glucose can inhibit xylose uptake rate of yl-XYL+*04*10 by 69.9% when using 30 g/L of xylose (Figure 5F). Generally, inhibition of xylose uptake by dG and D-glucose are concentration dependent. As the concentration of dG or D-glucose increases, the inhibition is significantly enhanced. Besides, inhibition of xylose uptake by D-glucose is more severe than that by dG.

Through the fermentation phenotype and xylose uptake kinetics analysis, we basically assumed that D-glucose/xylose co-fermentation phenotype of the evolved strains was closely related to xylose uptake enhancement (or weakened inhibition by D-glucose) and lower capacity to utilize D-glucose alone, but the genotype changes responsible for the phenotype is still not clear.

2.3. RNA-seq analysis

RNA-seq was performed to investigate the differences in global gene expression between strain yl-XYL+ and yl-XYL+*04*10. RNA was obtained after 6 h of fermentation in the D-glucose medium and D-glucose/xylose medium respectively. The number of genes significantly regulated (up-regulated by more than 2-fold or decreased by at least 50%) in yl-XYL+*04*10 in D-glucose and mixed sugar medium was 56 and 12, respectively; The ten most upregulated and downregulated genes in yl-XYL+*04*10 are listed in Table S2 and S3, respectively. For instance, the transcript levels of genes encoding taurine dioxygenase and malate synthase (YALI0_A21439g and YALI0_D19140g, respectively), were 13.1- and 8.2-fold higher in yl-XYL+*04*10. Transcription of YALI0_A21439g and YALI0_C23452g, which encodes a protein of

unknown function involved in serine/threonine metabolism, was enhanced by 11.3- and 5.0-fold. Besides, transcript levels of YALI0_D01111g encoding a D-glucose transporter decreased by 63%.

To figure out the putative genes directly responsible to D-glucose/xylose co-utilization, transcriptional level of genes involved in D-glucose and pentose metabolism were carefully investigated and the transcriptional profiling was shown along with metabolic pathway (Figure 6).

Generally, genes involved in hexose utilization including transport and catabolism was down-regulated, among which, genes YALI0_E20427g and YALI0_E20207g were even down-regulated by 67.9% and 35.2%, respectively (Figure 7A, E4G_vs_C0G). It explains to some extent why the rate of D-glucose utilization is reduced in mixed-sugar fermentation. On the contrary, several genes encoding pentose-specific transporters were dramatically up-regulated. For example, gene YALI0_D00363g and YALI0_C04730g were up-regulated by 60% and 3.52-fold, respectively (Figure 7C and D). Since YALI0_C04730g is also annotated as an arabinose-specific transporter, the fermentation phenotype of original and evolved strains in arabinose medium was investigated (Figure S3). We found that all strains cannot grow with arabinose with sole carbon source. However, the evolved strains can uptake arabinose in presence of D-glucose, and yl-XYL+*04*10 can even uptake 12.2 g/L arabinose within 48 h in $YPD_{15}A_{15}$, while yl-XYL+ cannot (Figure S3C).

Interestingly, not all the genes annotated as pentose-specific transporters were up-regulated, of which, YALI0_B00396g and YALI0_D01111g were down-regulated by 47.6% and 63% (Figure 7E and F, E4GX_vs_C0GX). This could suggest a misannotation of these transporter and further characterization of their real function in vivo would be required to verify this. Besides, genes involved in pentose phosphate pathway (PPP) such as *tkt* (YALI0_E06479g, encoding transketolase) and *tal* (YALI0_F15587g, encoding transaldolase) did not change expression level very much, which is unexpected. It seems that the major responsible changes for the improved uptake of xylose are at the level of transporters efficiency rather than PPP.

RNA-seq did not only reveal global changes in gene expression levels in evolved strains compared to the parent strain, but also helped us to identify meaningful mutations in some key genes (including base insertion, deletion or substitution) (Table S4). For example, a single nucleotide substitution occurred in gene YALI0_E23287g encoding a D-glucose transporter with adenine (A) replacing cytosine (C) at base 1118, which resulted in an amino acid residue change of N373T. Another important point mutation was found in YALI0_E15488g encoding a hexokinase with cytosine (C) replacing guanine (G) at base 809. The single base substitution lead to a codon change at amino acid 270 from glycine to alanine (G270A). We confirmed above point mutations using PCR amplification and subsequent DNA sequencing (Figure S4). However, we did not study the mutation probability of a certain gene at the population level, and the mutation law, because this article does not focus on this point. We hypothesize that such mutation could lead to a reduced use of D-glucose. In order to prove that, we then checked the hexokinase activity of the evolved strain yl-XYL+*04*10 and it resulted to be decreased by 73.4% and 74.4% in YPD_{30} medium

and $YPD_{30}X_{30}$ medium respectively, compared to the original strain (Figure 8). There was significant difference in the hexokinase activity of the evolved strain yl-XYL+*04*10 and the original strain (Figure 8). This explains, at least to some extent, why the utilization of D-glucose is weakened in the evolved strain.

3. DISCUSSION

In the study, we generated for the first time a strain of *Y. lipolytica* able to co-consume D-glucose and xylose, by using dG tolerance evolution. Here, we demonstrated a whole strain improvement cycle, which started with the evolution, continued with transcriptome analysis, and finalized with the identification of several novel potential gene targets for xylose transporter engineering. Our work provides a new approach for breeding *Y. lipolytica* and paved the way for improved pentose metabolic engineering.

For the original strain yl-XYL+, uptake rate of D-glucose and xylose are very similar when they are utilized alone; However, xylose uptake does not occur until D-glucose is exhausted, revealing that xylose transport or metabolism of is completely inhibited by D-glucose. On the contrary, the evolved strain yl-XYL+*04*10, can utilize 30 g/L D-glucose and xylose respectively in 36 h without obvious preference, but its D-glucose uptake rate was slightly decreased compared to yl-XYL+ in D-glucose/xylose medium (Figure 4). At the same time, we found that with the evolution continued, the biomass of evolved strain decreased, in agreement with previous observations [32, 33]. It is speculated that the decrease of biomass is mainly caused by changes of glucose and xylose metabolism in evolved strains. The enhanced xylose utilization with simultaneous weakened glucose utilization led to lower growth rate and final biomass production as growth rate of xylose-grown strains is generally somewhat lower than that of glucose-grown strains [34]. The results of sugar uptake kinetics and D-glucose/xylose fermentation dynamics suggested that yl-XYL+*04*10 obtained comparative advantage in xylose/D-glucose co-fermentation via derepressed xylose uptake at the expense of decreasing D-glucose utilization (Figure 5).

Decreased D-glucose uptake is an important feature of the evolved strain yl-XYL+*04*10. It could be mainly attributed to two reasons in our work. Firstly, transcript levels of many genes involved in hexose metabolism and transport decreased varying from 15.3% to 40.5% (Figure 7A and B). In addition, single-base substitution mutations were detected in hexokinase YALI0_E15488g and D-glucose transporter YALI0_E23287g (Table S4 and Figure S4). According to protein homology modeling, we speculated that the missense mutations N373T and G270A reduced the affinity of the transporter for glucose and the binding affinity of hexokinase to glucose (Figure S5), respectively, in agreement with the previous observations[35, 36], but detailed mechanism remained to be further studied; enzymatic data confirmed decreased hexokinase activity, which explained why D-glucose utilization slowed down in yl-XYL+*04*10 to some extent (Figure 8).

The phenotype of decreased D-glucose utilization have also been revealed in other microorganisms that underwent ALE with dG as competitor to xylose in medium [25-28, 32]. It suggests that it may be a universal mechanism for microorganisms to resist to dG

toxicity. Since dG cannot be metabolized to generate energy, microbe have to evolve to reduce energy consumption used to catalytically convert dG by down-regulating hexose metabolism pathway and hexokinase activity. Nonmetabolizable substrate substitution (i.e. dG replacing D-glucose), or hexose metabolism pathway blocking (deletion of hexokinase and glucokinase encoding genes), created the conditions to drive microorganism to evolve to transport and utilize xylose in the presence of D-glucose [24, 25, 27, 31]. Both of above evolutionary strategies have been applied in *S. cerevisiae* to obtain mutant transporters to transport D-xylose without inhibition by D-glucose or mutant strain which can co-utilize D-glucose and xylose [24, 29, 37], which maybe applicable to *Y. lipolytica*. However, it is still unclear whether the weakening of the hexose metabolism will positively lead the increase of xylose transport and catabolic rate.

Another feature of the evolved strain yl-XYL+*04*10 is that its xylose uptake is hardly inhibited by D-glucose or dG (Figure 5). Xylose uptake kinetics confirmed that its xylose uptake inhibition by D-glucose or dG had been partially relieved, so that its xylose uptake rate is increased by 2 orders of magnitude in the presence of D-glucose compared to the parent strain.

In addition, we compared the transcriptional level of genes involved in xylose utilization of the strains before and after evolution, and found that the they did not change significantly (Figure 6). In contrast, several genes encoding pentose transporter such as YALI0_C04730g and YALI0_D00363g were highly up-regulated (from 60% to 3.5-folds), indicating that xylose transport but not xylose metabolism contribute to xylose uptake enhancement (Figure 7). Therefore, D-glucose seems to inhibit xylose transport in yl-XYL+. Although the mechanism responsible to those genes up-regulation is not clear in *Y. lipolytica*, increasing xylose transporter expression in this study seems an effective strategy to promote xylose consumption in the presence of D-glucose.

Interestingly, not all genes annotated as pentose transporters are candidate gene targets for pentose engineering. We also noted that overexpression level of some genes such as YALI0_D01111g and YALI0_B00396g that have been previously annotated as pentose specific transporter even decreased by 47.6% and 48.8% in our evolved strains, respectively [16, 17, 21] (Figure 7). It suggests the complexity of pentose transporters inhibition and a necessity for the re-exploration and re-annotation of those transporter.

In previous studies, the xylose metabolic engineering of *Y. lipolytica* mainly focused on xylose pathway construction and the balance of cofactors [15, 17, 18, 20], with very little attention paid to sugar transporters engineering [16, 21]. Many transporter engineering strategies such as screening heterologous xylose-specific transporters and protein engineering of endogenous transporters have been adapted to promote D-glucose/xylose co-utilization [24, 38-42]. Such strategies could be transferable to *Y. lipolytica* and similarly, the approach discovered in this article could be used in *S.cerevisiae* and other organisms.

4. CONCLUSIONS

In the study, dG tolerance evolution was adapted to improve D-glucose/xylose co-

utilization by yl-XYL+, yielding an evolved strain yl-XYL+*04*10. The results of substrate uptake kinetics, transcriptomics, enzymology and genetic verification indicated that xylose-specific transporters YALI0_C04730g and YALI0_D00363g of yl-XYL+*04*10 and single-base substitution mutation in hexokinase YALI0_E15488g and D-glucose transporter YALI0_E23287g respectively (G270A and N373T) contribute to phenotype improvement. Our work paves the way for the improved utilization of lignocellulosic hydrolysates for the production of fuels and chemicals in *Y. lipolytica*.

5. MATERIALS AND METHODS

5.1. Strain and culture conditions

Y. lipolytica XYL+ (yl-XYL+) (overexpressing *ss*XR, *ss*XDH and *yl*XK) was used as parental strain[18]. YPX_{20} medium composing of 10 g/L yeast extract, 20 g/L peptone (AngelYeast Co., Ltd, China), and 20 g/L xylose was used for seed cultivation of yeasts. $YNBdG_xD_2X_{10}$ medium contains 1.7 g/L yeast nitrogen base (YNBww), 5 g/L NH_4Cl, 2 g/L D-glucose and 10 g/L xylose, which was used for evolutionary engineering by supplementing different amount of 2-deoxy-D-glucose (dG_x). $YNBD_{15}X_{15}$ medium (with 15 g/L D-glucose and 15 g/L xylose), $YNBD_{15}A_{15}$ medium (with 15 g/L D-glucose and 15 g/L arabinose), YPX_{30} medium (with 30 g/L xylose), YPD_{30} medium (with 30 g/L glucose) and $YPD_{30}X_{30}$ (with 30 g/L D-glucose and 30 g/L xylose) were used for fermentation phenotype test. Solid medium was prepared by adding 20 g/L agar. Yeast cells were cultivated in liquid media at 30 °C with a rotation of 250 rpm. All other chemicals used were from commercial source and were of reagent grade.

Typically, cultivation was performed as follows. A colony is picked up from a YPX_{20} plate and then inoculated into a 15 mL glass tube filled with 4 mL YPX_{20} liquid medium followed by cultivation for 16 h at 30 °C with 250 rpm. Cells were then collected to inoculate 50 mL YPX_{20} medium in 250 mL Erlenmeyer flasks making the initial OD_{600} was 0.1. The flasks were incubated at 30 °C, 250 rpm.

5.2. Evolutionary engineering

$YNBdG_xD_2X_{10}$ medium were used to domesticate yl-XYL+. In order to establish a domestication system, the effects of D-glucose analog 2-deoxyglucose (hereafter abbreviated as dG) lethality, initial OD_{600}, xylose and D-glucose concentration on yl-XYL+ were evaluated. Initial OD_{600} (0.1, 0.2, 0.5, 1 and 2), xylose concentration (10, 15, 20, 25 and 30 g/L), and D-glucose concentration (0, 0.5, 1, 2 and 5 g/L) were evaluated by single factor experiments.

The survival rate was calculated based on the following equations:

$$N_t = \frac{C}{V} \times M \qquad (1)$$

$$\text{Survival rate}(\%) = 1 - \frac{N_0 - N_t}{N_0} \times 100\% \qquad (2)$$

In equations above, N_t is the number of cells in the sample at t h; C is the average

number of colonies grown on a plate at a certain dilution ratio; V was the volume of the diluent used and M was the dilution factor.

The whole evolution process was divided into four stages, and 1, 2, 5 and 10 g/L of dG was added in the evolution medium respectively. Yl-XYL+ was cultured in tubes with $YNBdG_1D_2X_{10}$ medium (composing of 1 g/L dG, 2 g/L glucose and 10 g/L xylose) initially, sub-cultured every 48 h, and samples were taken for OD_{600} and xylose concentration determination. Every stage of domestication was ended until the residual xylose concentration was less than 0.5 g/L. Then the evolved strains were spread on plate and ten randomly colonies were picked up for phenotype test. The best one was selected for subsequent evolution.

5.3. Phenotypic testing of strains

Phenotypic testing was carried out in 250 mL Erlenmeyer flasks with a working volume of 50 mL at 30 °C with a rotation of 250 rpm. The cell pellets used for inoculation were obtained by centrifuging the seed culture at 4000 rpm for 5 min and the supernatant was discarded. The obtained cell pellets were used to inoculate fermentation medium with the initial OD_{600} set at 0.5. Samples for analysis were taken at regular intervals for analysis of OD_{600}, substrate and products concentration.

5.4. Xylose uptake kinetics in parent and evolved strains

Inhibitory effect of D-glucose and dG on xylose uptake is performed according to Farwick's procedure[19] with some modification. Cells were collected by centrifugation, washed for two times with ddH_2O and then resuspended to make OD_{600} reach around 60. The cells and substrates (Table1) were added to a pre-cooled 15 mL centrifuge tube with a volume ratio of 1:1. The reaction is kept at 30 °C, 250 rpm for 1 h. It is sampled every 15 min, and the sample was immediately placed on ice to terminate the reaction. At the end of the reaction, the sample was analyzed for xylose concentration using a high-performance liquid chromatography (HPLC). Referring to the Michaelis-Menten equation, the double reciprocal plot was used to determine the K_m and V_{max} [24, 43].

Table 1 Test groups and conditions of Xylose uptake kinetics

Group division	dG/G(g/L)	Xylose(mM)
A	0	20, 50, 100, 200, 500
B	1	20, 50, 100, 200, 500
C	2	20, 50, 100, 200, 500
D	5	20, 50, 100, 200, 500
E	10	20, 50, 100, 200, 500

5.5. RNA sequencing, gene expression, SNP analysis and Protein structure prediction

The cells were used to inoculate fermentation media with the initial fermentation OD_{600} set at 0.5. Fermentations were conducted for 48 h in a 250 mL flask with a

working volume of 50 mL at 30 °C, 250 rpm. Samples were taken at 6 h, and collected for liquid nitrogen preservation. The samples were ground with a mortar, and the disrupted cells were collected in a 1.5 mL centrifuge tube and then sealed with 1 mL of trizol. The samples were stored in dry ice and sent out. RNA isolation, library construction, sequencing were performed by Shanghai Shenggong Bioengineering Technology Service Co., Ltd using Illumina HiSeqTM 2500 as described previously [44, 45]. RNA-Seq data analysis including quality control, reads mapping, transcriptome assembly, annotation, gene expression level analysis and SNP calling are carried out according to previously published standard procedures [44, 45]. The raw data has been deposited in NCBI (SRA accession: PRJNA564077).

Quantitative Real-time PCR (qRT-PCR) was adapted to detect expression level of key genes and validate the corresponding results of RNA-seq. RNA isolation and cDNA synthesis are completed as previously described [46]. An Applied Biosystems StepOnePlus Real-Time PCR system (Thermo-Fisher Scientific Inc., Waltham, MA, USA) was used for RT-PCR. SYBR® Green Premix Ex TaqTM II kits (Takara, Dalian, Liaoning, China) was used under the following reaction conditions: 50 °C for 2 min, 95 °C for 2 min, followed by 40 cycles of 95 °C for 3 s, 60 °C for 30 s, and 72 °C for 30 s. All assays were performed at least in triplicate. All qRT-PCR primers are listed in Table S1.

Homology modeling of the YALI0_E23287g (encoding a D-glucose transporter) and YALI0_E15488g (encoding a hexokinase) were performed using the SWISS-MODEL server (https://swissmodel.expasy.org/) [47]. The model of the sugar transport protein STP10 (PDB: 6h7d) and hexokinase-1(PDB: 3b8a) were chosen as template, respectively. 3D model was assessed and colored using Pymol (The PyMOL Molecular Graphics System, Version 2.1.1 Schrödinger, LLC.).

5.6. Analytical methods

The amounts of sugars and organic acids of hydrolysis and fermentation samples were analyzed by HPLC equipped with a Bio-rad Aminex HPX-87H column and a refractive index detector. The Aminex HPX-87P column was maintained at 30 °C, the mobile phase was 0.005 M sulfuric acid at 65 °C with a flow rate of 0.6 mL/min [48]. All liquid samples were filtered and kept refrigerated at 4 °C until analyzed. Concentrations of monomeric sugars were calculated based on the calibration sugar standards and shown as an average value of three parallel samples. Biomass formation was quantified by measuring optical density (OD) at 600 nm using a UV-visible spectrophotometer (TU-1810, Beijing pushen general instrument co., LTD). The analyses of hexokinase (HK) was performed using Hexokinase (HK) activity assay kit (Beijing Solarbio Science & Technology Co., Ltd) following manufacturer's instructions.

The preprint of this article had been posted on Research Square [48].

ASSOCIATED CONTENT

Supporting Information

Supporting information for Supplementary Figure S1-6 and Supplementary Table S1-

4.

AUTHOR INFORMATION

Corresponding Author
Email: jinmingjie@njust.edu.cn; zqwen@njust.edu.cn
ORCID
Jin Mingjie: 0000-0002-9493-305X
Wen Zhiqiang: 0000-0001-8083-7588

Author Contributions

Linlin Zhou, Zhiqiang Wen, Zedi Wang, and Yuwei Zhang performed the experiments, and analyzed the data; Zhiqiang Wen and Mingjie Jin coordinated and supervised this study; Linlin Zhou, Zhiqiang Wen, Mingjie Jin and Rodrigo Ledesma-Amaro drafted and revised the manuscript.

Funding

This work was supported by "Natural Science Foundation of Jiangsu Province", Grant No. BK20170037, "National Key R&D Program of China", Grant No. 2016YFE0105400, "National Natural Science Foundation of China", Grant Nos. 21606132 & 21706133, and "The Fundamental Research Funds for the Central Universities", Grant Nos.30916011202 & 30918011310.

Conflict of interest

The authors declare no financial or commercial conflict of interest.

REFERENCES

(1) Ledesma-Amaro, R.; Nicaud, J.-M. Metabolic Engineering for Expanding the Substrate Range of Yarrowia lipolytica. Trends Biotechnol. **2016,** 34, 798-809.
(2) Sabra, W.; Bommareddy, R. R.; Maheshwari, G.; Papanikolaou, S.; Zeng, A.-P. Substrates and oxygen dependent citric acid production by Yarrowia lipolytica: insights through transcriptome and fluxome analyses. Microb. cell fact. **2017,** 16, 78.
(3) Zinjarde, S.; Apte, M.; Mohite, P.; Kumar, A. R. Yarrowia lipolytica and pollutants: Interactions and applications. Biotechnol. Adv. **2014,** 32, 920-933.
(4) Gao, S.; Tong, Y.; Zhu, L.; Ge, M.; Zhang, Y.; Chen, D.; Jiang, Y.; Yang, S. Iterative integration of multiple-copy pathway genes in Yarrowia lipolytica for heterologous beta-carotene production. Metab. Eng. **2017,** 41, 192-201.
(5) Beneyton, T.; Thomas, S.; Griffiths, A. D.; Nicaud, J.-M.; Drevelle, A.; Rossignol, T. Droplet-based microfluidic high-throughput screening of heterologous enzymes secreted by the yeast Yarrowia lipolytica. Microb. cell fact. **2017,** 16, 18.
(6) Qiao, K.; Abidi, S. H. I.; Liu, H.; Zhang, H.; Chakraborty, S.; Watson, N.; Ajikumar, P. K.; Stephanopoulos, G. Engineering lipid overproduction in the oleaginous yeast Yarrowia lipolytica. Metab. Eng. **2015,** 29, 56-65.
(7) Liu, H.; Marsafari, M.; Wang, F.; Deng, L.; Xu, P. Engineering acetyl-CoA metabolic shortcut for eco-friendly production of polyketides triacetic acid lactone in Yarrowia lipolytica. Metab. Eng. **2019,** 56, 60-68.
(8) Zhou, Y. J.; Buijs, N. A.; Siewers, V.; Nielsen, J. Fatty Acid-Derived Biofuels and Chemicals Production in Saccharomyces cerevisiae. Front. Bioeng. Biotech. **2014,** 2, 32.
(9) Wu, H.; San, K. Y. Efficient odd straight medium chain free fatty acid production by metabolically engineered Escherichia coli. Biotechnol. Bioeng. **2014,** 111, 2209-2219.
(10) Yu, T.; Zhou, Y.J.; Huang, M.; Liu, Q.; Pereira, R.; David, F.; Nielsen, J. Reprogramming yeast metabolism from alcoholic fermentation to lipogenesis. Cell **2018**, 174, 1549-1558.
(11) Qiao, K.; Wasylenko, T. M.; Zhou, K.; Xu, P.; Stephanopoulos, G. Lipid production in Yarrowia lipolytica is maximized by engineering cytosolic redox metabolism. Nat. Biotechnol. **2017,** 35, 173-177.
(12) Xu, P.; Qiao, K.; Ahn, W. S.; Stephanopoulos, G. Engineering Yarrowia lipolytica as a platform for synthesis of drop-in transportation fuels and oleochemicals. Proc. Natl. Acad. Sci. U. S. A. **2016,** 113, 10848-10853.
(13) Xu, P.; Qiao, K.; Stephanopoulos, G. Engineering oxidative stress defense pathways to build a robust lipid production platform in Yarrowia lipolytica. Biotechnol. Bioeng. **2017,** 114, 1521-1530.
(14) Jin, M.; Slininger, P. J.; Dien, B. S.; Waghmode, S.; Moser, B. R.; Orjuela, A.; Sousal, L. d. C.; Balan, V. Microbial lipid-based lignocellulosic biorefinery: feasibility and challenges. Trends Biotechnol. **2015,** 33, 43-54.
(15) Niehus, X.; Crutz-Le Coq, A.-M.; Sandoval, G.; Nicaud, J.-M.; Ledesma-Amaro, R. Engineering Yarrowia lipolytica to enhance lipid production from lignocellulosic materials. Biotechnol. Biofuels **2018,** 11, 11.
(16) Ryu, S.; Trinh, C. T. Understanding Functional Roles of Native Pentose-Specific Transporters for Activating Dormant Pentose Metabolism in Yarrowia lipolytica. Appl. Environ. Microbiol. **2018,** 84, UNSP e02146-17.
(17) Spagnuolo, M.; Hussain, M. S.; Gambill, L.; Blenner, M. Alternative Substrate Metabolism in

Yarrowia lipolytica. Front. Microbiol. **2018,** 9, 1077.
(18) Ledesma-Amaro, R.; Lazar, Z.; Rakicka, M.; Guo, Z.; Fouchard, F.; Crutz-Le Coq, A.-M.; Nicaud, J.-M. Metabolic engineeringof Yarrowia lipolytica to produce chemicals and fuels from xylose. Metab. Eng. **2016,** 38, 115-124.
(19) Li, H.; Alper, H. S. Enabling xylose utilization in Yarrowia lipolytica for lipid production. Biotechnol. J. **2016,** 11, 1230-1240.
(20) Rodriguez, G. M.; Hussain, M. S.; Gambill, L.; Gao, D.; Yaguchi, A.; Blenner, M. Engineering xylose utilization in Yarrowia lipolytica by understanding its cryptic xylose pathway. Biotechnol. Biofuels **2016,** 9, 149.
(21) Ryu, S.; Hipp, J.; Trinh, C. T. Activating and Elucidating Metabolism of Complex Sugars in Yarrowia lipolytica. Appl. Environ. Microbiol. **2016,** 82, 1334-1345.
(22) Goerke, B.; Stuelke, J. Carbon catabolite repression in bacteria: many ways to make the most out of nutrients. Nat. Rev. Microbiol. **2008,** 6, 613-624.
(23) Bruder, M.; Moo-Young, M.; Chung, D. A.; Chou, C. P. Elimination of carbon catabolite repression in Clostridium acetobutylicum-a journey toward simultaneous use of xylose and glucose. Appl. Microbiol. Biotechnol. **2015,** 99, 7579-7588.
(24) Farwick, A.; Bruder, S.; Schadeweg, V.; Oreb, M.; Boles, E. Engineering of yeast hexose transporters to transport D-xylose without inhibition by D-glucose. Proc. Natl. Acad. Sci. U. S. A. **2014,** 111, 5159-5164.
(25) Lane, S.; Xu, H.; Oh, E. J.; Kim, H.; Lesmana, A.; Jeong, D.; Zhang, G.; Tsai, C.-S.; Jin, Y.-S.; Kim, S. R. Glucose repression can be alleviated by reducing glucose phosphorylation rate in Saccharomyces cerevisiae. Sci. Rep. **2018,** 8, 2613.
(26) Dashtban, M.; Wen, X.; Bajwa, P. K.; Ho, C.-Y.; Lee, H. Deletion of hxk1 gene results in derepression of xylose utilization in Scheffersomyces stipitis. J. Ind. Microbiol. Biotechnol. **2015,** 42, 889-896.
(27) Mohagheghi, A.; Linger, J.; Smith, H.; Yang, S.; Dowe, N.; Pienkos, P. T. Improving xylose utilization by recombinant Zymomonas mobilis strain 8b through adaptation using 2-deoxyglucose. Biotechnol. Biofuels **2014,** 7, 19.
(28) Sreenath, H. K.; Jeffries, T. W. 2-deoxyglucose as a selective agent for derepressed mutants of Pichia stipitis. Appl. Biochem. Biotechnol. **1999,** 77-9, 211-222.
(29) Kahar, P.; Taku, K.; Tanaka, S. Enhancement of xylose uptake in 2-deoxyglucose tolerant mutant of Saccharomyces cerevisiae. J. Biosci. Bioeng. **2011,** 111, 557-563.
(30) Li, H.; Alper, H. S. Producing Biochemicals in Yarrowia lipolytica from Xylose through a Strain Mating Approach. Biotechnol. J. **2020,** 15, 1900304.
(31) Zhu, M.; Lu, Y.; Wang, J.; Li, S.; Wang, X. Carbon Catabolite Repression and the Related Genes of ccpA, ptsH and hprK in Thermoanaerobacterium aotearoense. PLoS One **2015,** 10, e0142121.
(32) Kim, S. B.; Kwon, D. H.; Park, J. B.; Ha, S. J. Alleviation of catabolite repression in Kluyveromyces marxianus: the thermotolerant SBK1 mutant simultaneously coferments glucose and xylose. Biotechnol. Biofuels **2019,** 12, 90.
(33) Suprayogi, S.; Nguyen, M. T.; Lertwattanasakul, N.; Rodrussamee, N.; Limtong, S.; Kosaka, T.; Yamada, M. A Kluyveromyces marxianus 2-deoxyglucose-resistant mutant with enhanced activity of xylose utilization. Int. Microbiol. **2015,** 18, 235-244.
(34) Tiukova, I. A.; Brandenburg, J.; Blomqvist, J.; Sampels, S.; Mikkelsen, N.; Skaugen, M.; Arntzen, M. O.; Nielsen, J.; Sandgren, M.; Kerkhoven, E. J. Proteome analysis of xylose metabolism in

Rhodotorula toruloides during lipid production. Biotechnol. Biofuels **2019,** 12, 137.
(35) Paulsen, P. A., Custódio, Tânia F., & Pedersen, Bjørn Panyella. Crystal structure of the plant symporter stp10 illuminates sugar uptake mechanism in monosaccharide transporter superfamily. Nat. Commun. **2019**, 10, 407.
(36) Kuser, P.; Cupri, F.; Bleicher, L.; Polikarpov, I. Crystal structure of yeast hexokinase PI in complex with glucose: A classical "induced fit" example revised. Proteins. **2008,** 72, 731-740.
(37) Souto-Maior, A. M.; Runquist, D.; Hahn-Hagerdal, B. Crabtree-negative characteristics of recombinant xylose-utilizing Saccharomyces cerevisiae. J. Biotechnol. **2009,** 143, 119-123.
(38) Nijland, J. G.; Shin, H. Y.; de Jong, R. M.; De Waal, P. P.; Klaassen, P.; Driessen, A. J. M. Engineering of an endogenous hexose transporter into a specific D-xylose transporter facilitates glucose-xylose co-consumption in Saccharomyces cerevisiae. Biotechnol. Biofuels **2014,** 7, 168.
(39) Wang, C. Q.; Bao, X. M.; Li, Y. W.; Jiao, C. L.; Hou, J.; Zhang, Q. Z.; Zhang, W. X.; Liu, W. F.; Shen, Y. Cloning and characterization of heterologous transporters in Saccharomyces cerevisiae and identification of important amino acids for xylose utilization. Metab. Eng. **2015,** 30, 79-88.
(40) Young, E. M.; Comer, A. D.; Huang, H.; Alper, H. S. A molecular transporter engineering approach to improving xylose catabolism in Saccharomyces cerevisiae. Metab. Eng. **2012,** 14, 401-411.
(41) Young, E. M.; Tong, A.; Bui, H.; Spofford, C.; Alper, H. S. Rewiring yeast sugar transporter preference through modifying a conserved protein motif. Proc. Natl. Acad. Sci. U. S. A. **2014,** 111, 131-136.
(42) Apel, A. R.; Ouellet, M.; Szmidt-Middleton, H.; Keasling, J. D.; Mukhopadhyay, A. Evolved hexose transporter enhances xylose uptake and glucose/xylose co-utilization in Saccharomyces cerevisiae. Sci. Rep. **2016,** 6, 19512.
(43) Lee, W. J.; Kim, M. D.; Ryu, Y. W.; Bisson, L. F.; Seo, J. H. Kinetic studies on glucose and xylose transport in Saccharomyces cerevisiae. Appl. Microbiol. Biotechnol. **2002,** 60, 186-191.
(44) Wei, L.; Cao, L.; Miao, Y.; Wu, S.; Xu, S.; Wang, R.; Du, J.; Liang, A.; Fu, Y. Transcriptome analysis of Spodoptera frugiperda 9 (Sf9) cells infected with baculovirus, AcMNPV or AcMNPV-BmK IT. Biotechnol. Lett. **2017,** 39, 1129-1139.
(45) Wu, Y. H.; Wang, T.; Wang, K.; Liang, Q. Y.; Bai, Z. Y.; Liu, Q. L.; Pan, Y. Z.; Jiang, B. B.; Zhang, L. Comparative Analysis of the Chrysanthemum Leaf Transcript Profiling in Response to Salt Stress. PLoS One **2016,** 11, e0159721.
(46) Wen, Z.; Wu, M.; Lin, Y.; Yang, L.; Lin, J.; Cen, P. Artificial symbiosis for acetone-butanol-ethanol (ABE) fermentation from alkali extracted deshelled corn cobs by co-culture of Clostridium beijerinckii and Clostridium cellulovorans. Microb. Cell Fact. **2014,** 13, 1-11.
(47) Biasini, M.; Bienert, S.; Waterhouse, A.; Arnold, K.; Studer, G.; Schmidt, T.; Kiefer, F.; Gallo Cassarino, T.; Bertoni, M.; Bordoli, L.; Schwede, T. SWISS-MODEL: modelling protein tertiary and quaternary structure using evolutionary information. Nucleic Acids Res. **2014,** 42, W252-258.
(48) Chen, S.; Xu, Z.; Li, X.; Yu, J.; Cai, M.; Jin, M. Integrated bioethanol production from mixtures of corn and corn stover. Bioresour. Technol. **2018,** 258, 18-25.
(48) Zhou, L.; Wen, Z.; Wang, Z.; Zhang, Y.; Ledesma-Amaro, R.; Jin, M. Evolutionary engineering improved D-glucose/xylose co-fermentation of Yarrowia lipolytica. **2019,** DOI:10.21203/rs.2.19486/v1. Research Square. https://doi.org/10.21203/rs.2.19486/v1. (accessed Dec 20, 2019).

Figure Captions

Figure 1. Schematic representation of adaptive laboratory evolution (ALE) and transcriptional profiling. 1, Principle of 2-Deoxy-glucose (dG) tolerance evolution: dG similar to glucose in structure inhibiting xylose metabolism; 2, Four stages of ALE with increasing the concentration of dG from 1 g/L to 2, 5, 10 g/L; 3, Characterization of evolves strains by growth and fermentation; 4. Transcriptional profiling;5. Gene targets identification; G and X represent glucose and xylose, respectively.

Figure 2. Initial ALE condition test for yl-XYL+ in YNB medium. (A) Effect of dG on survival rate of yl-XYL+ in $YNBdG_{10}$ and $YNBdG_{10}X_{10}$ medium;(B) Effect of glucose addition on yl-XYL+ growth in $YNBD_xX_{10}$ medium ;(C) Effect of initial xylose concentration on xylose consumption within 24 hours in YNBX medium;(D) Effect of initial OD_{600} on xylose consumption within 24 hours in $YNBX_{10}$ medium. Each value indicates the average ± SD of biological replicates.

Figure 3. Mutants with derepressed pentose metabolism are obtained by adaptive laboratory evolution of strain yl-XYL+ in medium composing of xylose and 2-deoxyglucose (dG). **A**, ALE process of yl-XYL+ in $YNBdG_xX_{10}$ medium adding 2 g/L glucose. **Stage 1**: $YNBD_2dG_1X_{10}$ medium; **Stage 2**: $YNBD_2dG_2X_{10}$ medium; **Stage 3**: $YNBD_2dG_5X_{10}$ medium; **Stage 4**: $YNBD_2dG_{10}X_{10}$ medium; **B**, comparison of strains fermentation phenotypes in $YNBD_{15}X_{15}$ medium, in which 0, 1, 2, 3, 4 represent parent strain yl-XYL+ and 4 mutants selected at the end of each evolution stage (yl-XYL+*01*3, yl-XYL+*02*9, yl-XYL+*03*5 and yl-XYL+*04*10). Each value indicates the average ± SD of biological replicates.

Figure 4. Fermentation profile of yl-XYL+, yl-XYL+*01*3, and yl-XYL+*04*10 in YPD_{30}, YPX_{30}, and $YPD_{30}X_{30}$ medium for 48h. Cell growth (square) and the amount of glucose (circular) and xylose (triangle) residual in the media containing 30 g/L glucose (A, D and G), 30 g/L xylose (B, E and H) and 30 g/L glucose and 30 g/L xylose (C, F and I) were monitored. The shadow in third column (C, F, I) represents the difference in glucose and xylose utilization rates to a certain extent. Each value indicates the average ± SD of triplicate experiments.

Figure 5. Xylose uptake kinetics of yl-XYL+, yl-XYL+*01*3, and yl-XYL+*04*10 in $YNBdG_xX_x$ (A, B, C) and $YNBD_xX_x$ (D, E, F) medium respectively. 0dG, 1dG, 2dG, 5dG, 10dG represent 0, 1, 2, 5, 10 g/L of 2-deoxyglucose (dG), respectively; 0G, 1G, 2G, 5G, 10G represent 0, 1, 2, 5, 10 g/L of glucose, respectively. Each value indicates the average ± SD of biological replicates.

Figure 6. RNA-seq analysis of yl-XYL+*04*10 on sugar metabolism in YPD_{30} and $YPD_{30}X_{30}$ medium compared to yl-XYL+. Genes transcriptional profiling and mutation were shown along with sugar metabolic pathway. Expression level change of genes involved in glucose transportation & metabolism was measured in YPD_{30} medium, namely E4G_vs_E0G (displayed as genes-folds); Expression level change of genes involved in xylose or arabinose transportation & metabolism was measured in

$YPD_{30}X_{30}$ medium, namely E4GX_vs_E0GX (displayed as genes-folds). **Bold red font**, up-regulated by over 2 folds; Red font, moderately up-regulated; **Bold blue font**, down-regulated by over 50%; Blue font, moderately down-regulated; *(N373T) and *(G270A) represent amino acids missense mutation in YALI0_E23287g and YALI0_E15488g. XlyT, xylose transporter; XYR, xylose reductase; XDH, xylitol dehydrogenase; XKS, xylulokinase; AraT, arabinose transporter; AraA, L-arabinose isomerase; AraB, L-ribulose kinase; AraD, L-ribulose-5-phosphate 4-epimerase; LarA, L-arabinose reductase; LadA, L-arabinitol dehydrogenase; ALX, L-xylulose reductase; rpi, 5-phosphate ribose isomerase; Tkt, transketolase; Tal, transaldolase; GlcT, glucose transporter; Hk, hexokinase; Gpi, glucose-6-phosphate isomerase; Pfk, 6-phosphofructokinase; Fba, fructose-bisphosphate aldolase; Gapdh, glyceraldehyde 3-phosphate dehydrogenase; tpi, triosephosphate isomerase.

Figure 7. Transcriptional level analysis of key genes involved in sugar transportation & metabolism of yl-XYL+*01*3, and yl-XYL+*04*10 compared to yl-XYL+. (A), (B), transcriptional level change of genes involved in glucose transportation & metabolism in YPD_{30} medium (containing 30 g/L glucose), namely, E4G_vs_E0G and E1G_vs_C0G (indicated by RNA-seq); (C), (D), (E), (F), qRt-PCR confirmed transcriptional level of YALI0_D00363g, YALI0_C04730g, YALI0_D01111g and YALI0_B00396g, respectively in $YPD_{30}X_{30}$ medium (containing 30 g/L glucose and 30 g/L xylose), namely, E4GX_vs_C0GX and E1GX_vs_C0GX. Each value indicates the average ± SD of biological replicates.

Figure 8. Hexokinase activity of the original and evolved strains in YPD_{30} medium (A) and $YPD_{30}X_{30}$ medium (B). Each value indicates the average ± SD of biological replicates. (***, $P \leq 0.001$; **, $P \leq 0.01$; *, $P \leq 0.05$; NS, $P > 0.05$; *t*-test).

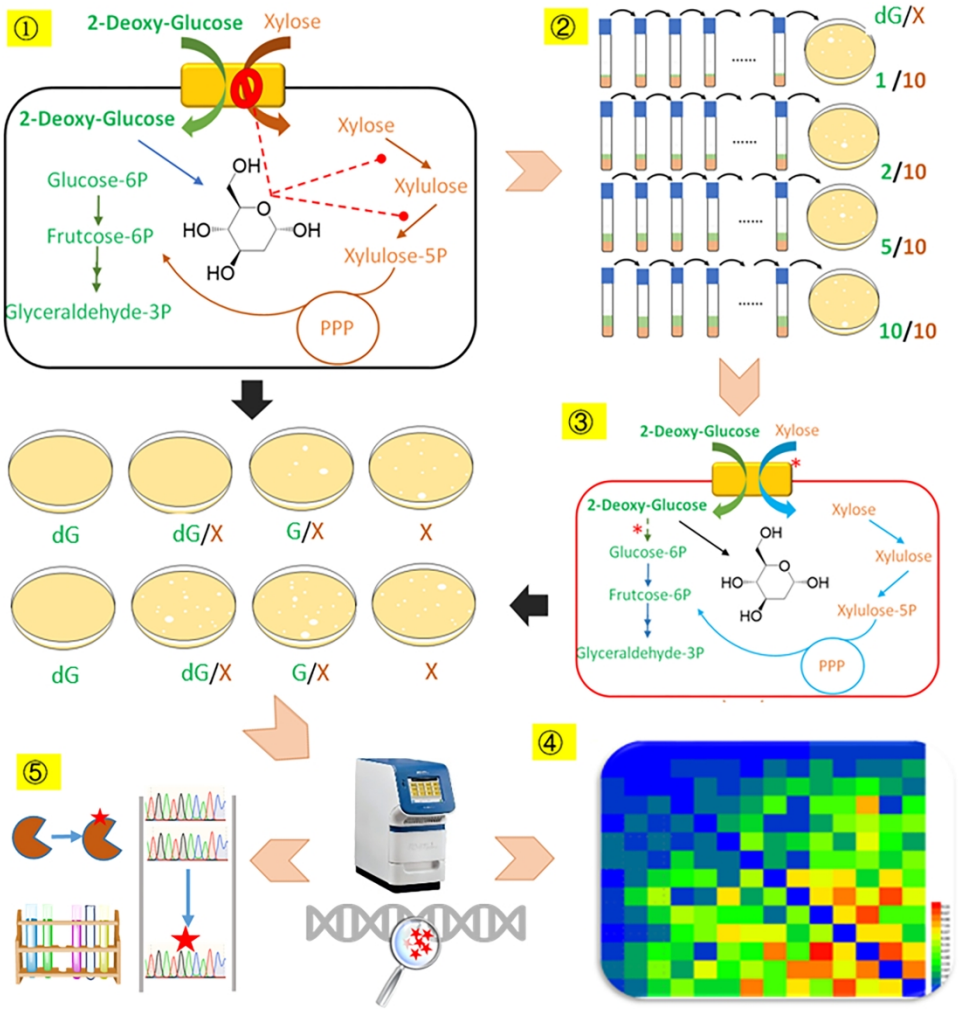

Figure 1. Schematic representation of adaptive laboratory evolution (ALE) and transcriptional profiling. 1, Principle of 2-Deoxy-glucose (dG) tolerance evolution: dG similar to glucose in structure inhibiting xylose metabolism; 2, Four stages of ALE with increasing the concentration of dG from 1 g/L to 2, 5, 10 g/L; 3, Characterization of evolves strains by growth and fermentation; 4. Transcriptional profiling;5. Gene targets identification; G and X represent glucose and xylose, respectively.

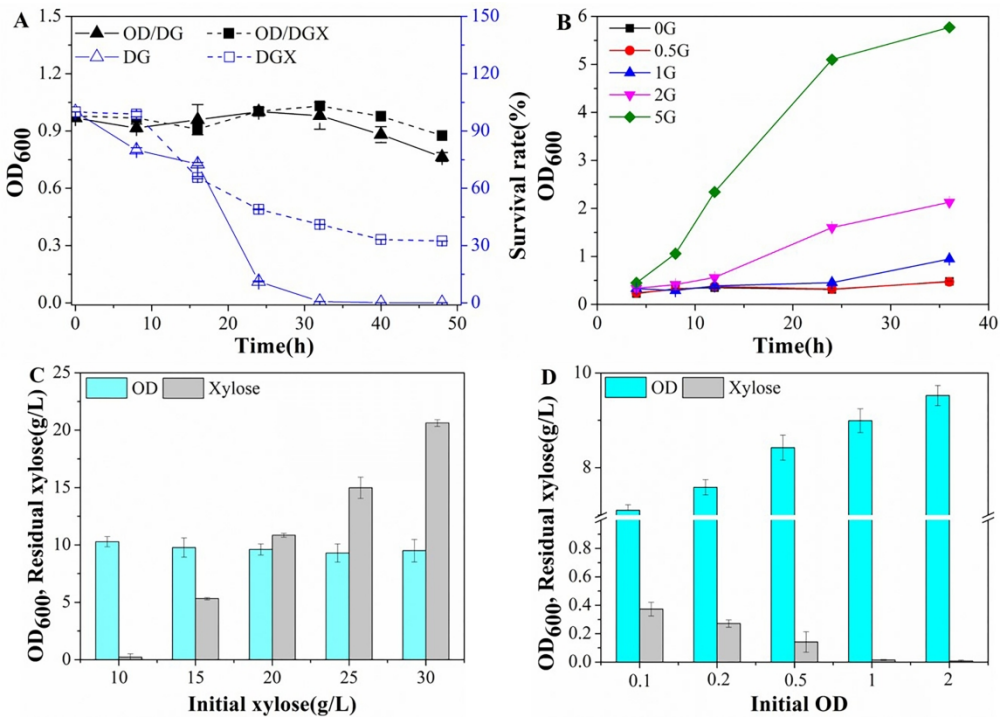

Figure 2. Initial ALE condition test for yl-XYL+ in YNB medium. (A) Effect of dG on survival rate of yl-XYL+ in YNBdG10 and YNBdG10X10 medium;(B) Effect of glucose addition on yl-XYL+ growth in YNBDxX10 medium ;(C) Effect of initial xylose concentration on xylose consumption within 24 hours in YNBX medium;(D) Effect of initial OD600 on xylose consumption within 24 hours in YNBX10 medium. Each value indicates the average ± SD of biological replicates.

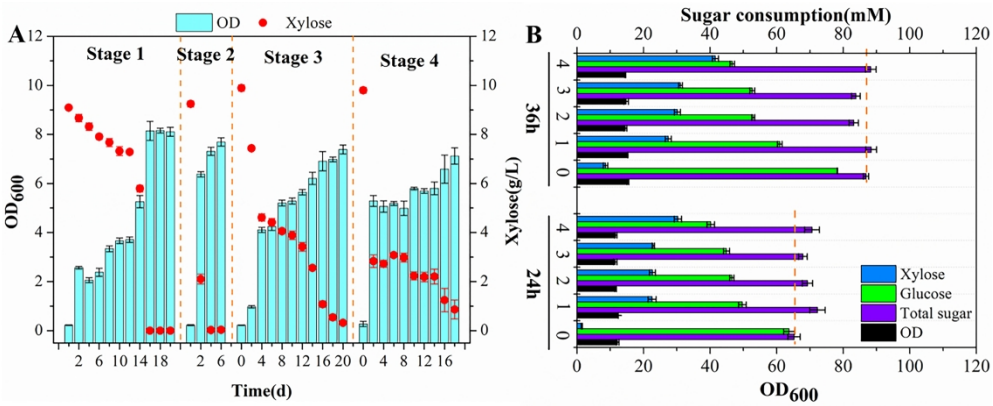

Figure 3. Mutants with derepressed pentose metabolism are obtained by adaptive laboratory evolution of strain yl-XYL+ in medium composing of xylose and 2-deoxyglucose (dG). A, ALE process of yl-XYL+ in YNBdGxX10 medium adding 2 g/L glucose. Stage 1: YNBD2dG1X10 medium; Stage 2: YNBD2dG2X10 medium; Stage 3: YNBD2dG5X10 medium; Stage 4: YNBD2dG10X10 medium; B, comparison of strains fermentation phenotypes in YNBD15X15 medium, in which 0, 1, 2, 3, 4 represent parent strain yl-XYL+ and 4 mutants selected at the end of each evolution stage (yl-XYL+*01*3, yl-XYL+*02*9, yl-XYL+*03*5 and yl-XYL+*04*10). Each value indicates the average ± SD of biological replicates.

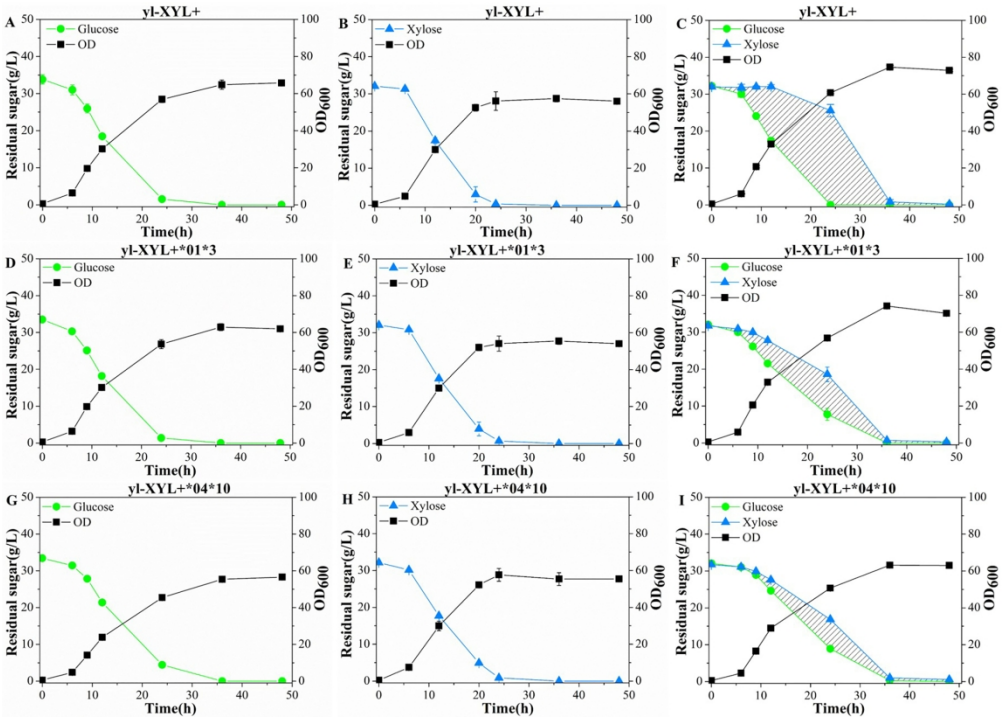

Figure 4. Fermentation profile of yl-XYL+, yl-XYL+*01*3, and yl-XYL+*04*10 in YPD30, YPX30, and YPD30X30 medium for 48h. Cell growth (square) and the amount of glucose (circular) and xylose (triangle) residual in the media containing 30 g/L glucose (A, D and G), 30 g/L xylose (B, E and H) and 30 g/L glucose and 30 g/L xylose (C, F and I) were monitored. The shadow in third column (C, F, I) represents the difference in glucose and xylose utilization rates to a certain extent. Each value indicates the average ± SD of triplicate experiments.

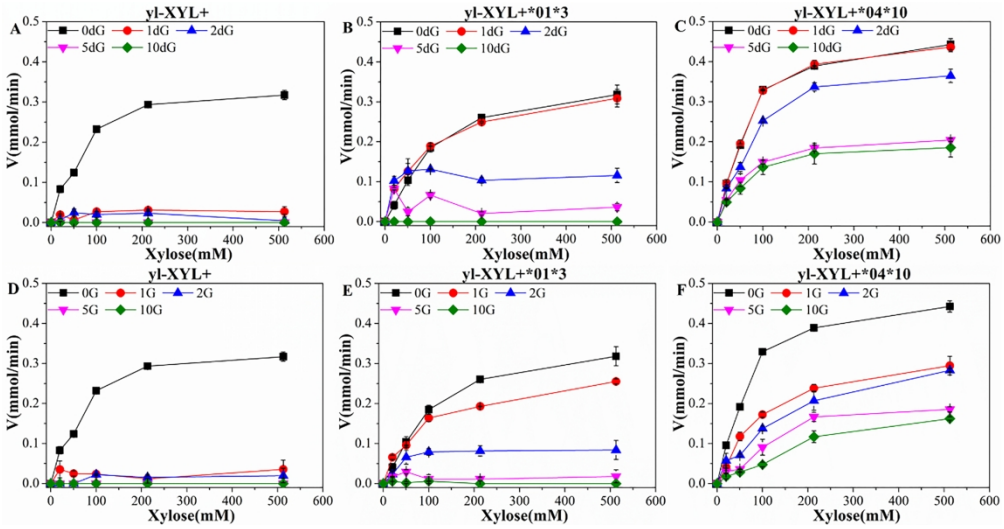

Figure 5. Xylose uptake kinetics of yl-XYL+, yl-XYL+*01*3, and yl-XYL+*04*10 in YNBdGxXx (A, B, C) and YNBDxXx (D, E, F) medium respectively. 0dG, 1dG, 2dG, 5dG, 10dG represent 0, 1, 2, 5, 10 g/L of 2-deoxyglucose (dG), respectively; 0G, 1G, 2G, 5G, 10G represent 0, 1, 2, 5, 10 g/L of glucose, respectively. Each value indicates the average ± SD of biological replicates.

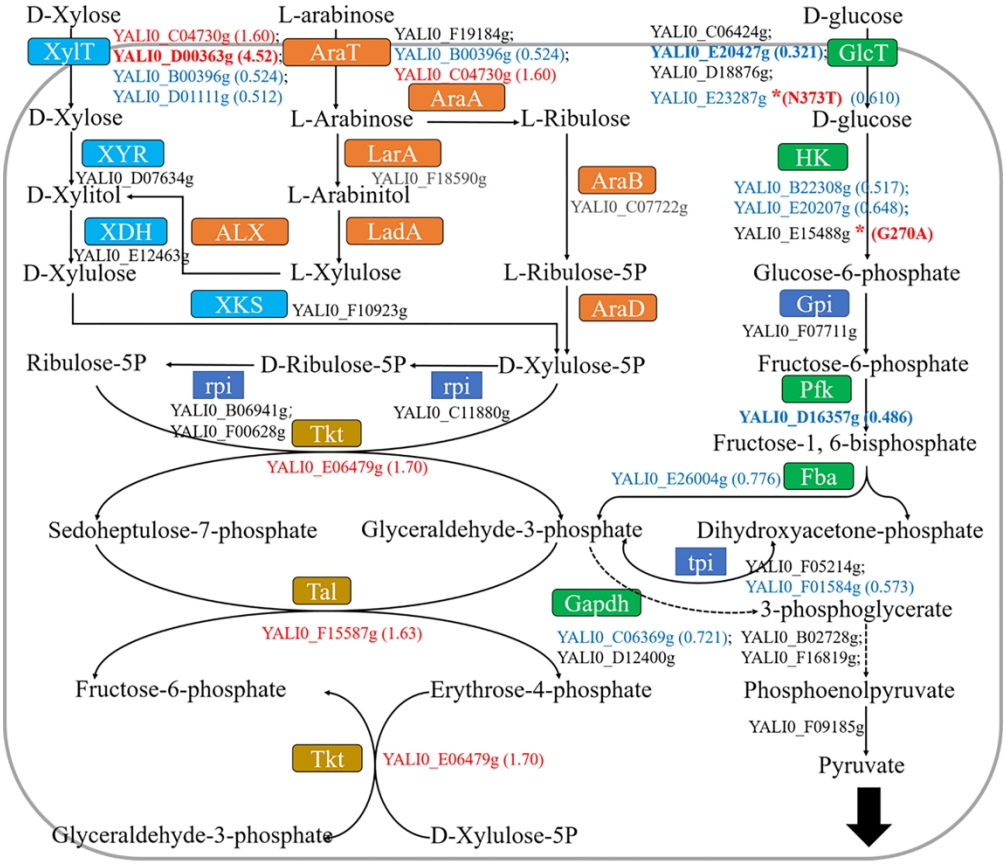

Figure 6. RNA-seq analysis of yl-XYL+*04*10 on sugar metabolism in YPD30 and YPD30X30 medium compared to yl-XYL+. Genes transcriptional profiling and mutation were shown along with sugar metabolic pathway. Expression level change of genes involved in glucose transportation & metabolism was measured in YPD30 medium, namely E4G_vs_E0G (displayed as genes-folds); Expression level change of genes involved in xylose or arabinose transportation & metabolism was measured in YPD30X30 medium, namely E4GX_vs_E0GX (displayed as genes-folds). Bold red font, up-regulated by over 2 folds; Red font, moderately up-regulated; Bold blue font, down-regulated by over 50%; Blue font, moderately down-regulated; *(N373T) and *(G270A) represent amino acids missense mutation in YALI0_E23287g and YALI0_E15488g. XlyT, xylose transporter; XYR, xylose reductase; XDH, xylitol dehydrogenase; XKS, xylulokinase; AraT, arabinose transporter; AraA, L-arabinose isomerase; AraB, L-ribulose kinase; AraD, L-ribulose-5-phosphate 4-epimerase; LarA, L-arabinose reductase; LadA, L-arabinitol dehydrogenase; ALX, L-xylulose reductase; rpi, 5-phosphate ribose isomerase; Tkt, transketolase; Tal, transaldolase; GlcT, glucose transporter; Hk, hexokinase; Gpi, glucose-6-phosphate isomerase; Pfk, 6-phosphofructokinase; Fba, fructose-bisphosphate aldolase; Gapdh, glyceraldehyde 3-phosphate dehydrogenase; tpi, triosephosphate isomerase.

160x139mm (600 x 600 DPI)

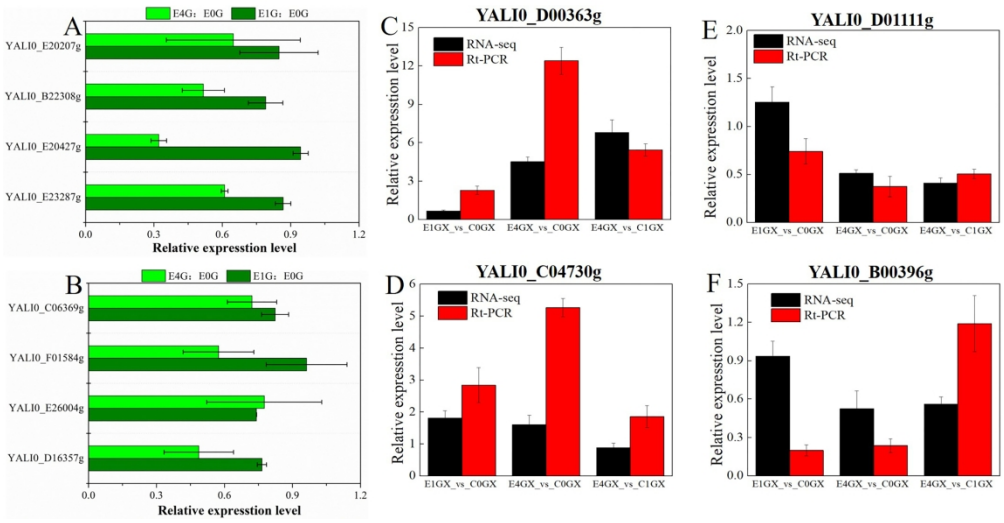

Figure 7. Transcriptional level analysis of key genes involved in sugar transportation & metabolism of yl-XYL+*01*3, and yl-XYL+*04*10 compared to yl-XYL+. (A), (B), transcriptional level change of genes involved in glucose transportation & metabolism in YPD30 medium (containing 30 g/L glucose), namely, E4G_vs_E0G and E1G_vs_C0G (indicated by RNA-seq); (C), (D), (E), (F), qRt-PCR confirmed transcriptional level of YALI0_D00363g, YALI0_C04730g, YALI0_D01111g and YALI0_B00396g, respectively in YPD30X30 medium (containing 30 g/L glucose and 30 g/L xylose), namely, E4GX_vs_C0GX and E1GX_vs_C0GX. Each value indicates the average ± SD of biological replicates.

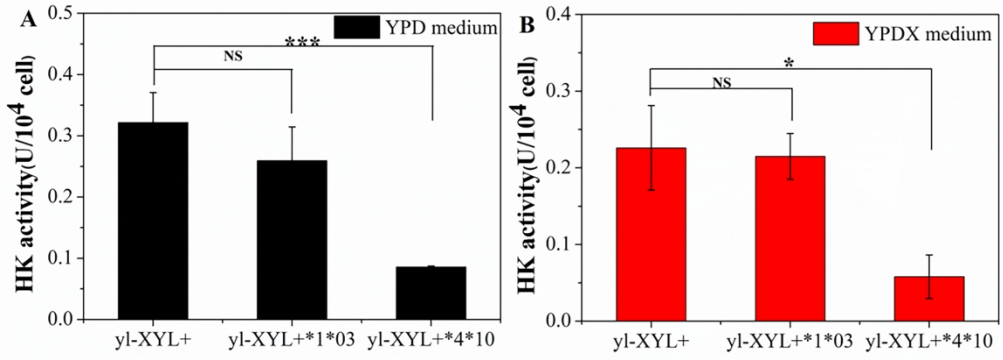

Figure 8. Hexokinase activity of the original and evolved strains in YPD30 medium (A) and YPD30X30 medium (B). Each value indicates the average ± SD of biological replicates. (***, P≤0.001; **, P≤0.01; *, P≤0.05; NS, P > 0.05; t-test).

160x58mm (600 x 600 DPI)